

000 REINFORCEMENT REWARD MODEL WITH POLICY 001 FEEDBACK 002

003 **Anonymous authors**

004 Paper under double-blind review

005 ABSTRACT

006 Reinforcement Learning from Human Feedback (RLHF) is a pivotal technique for
007 aligning large language models (LLMs) with human preferences, yet it is suscepti-
008 ble to reward hacking, a phenomenon that policy models exploit spurious reward
009 patterns instead of faithfully capturing human intent. Prior work to mitigate reward
010 hacking primarily relies on surface semantic information and fails to efficiently
011 address the misalignment between the reward model and the policy model caused
012 by continuous policy distribution shifts. This inevitably leads to an increasing
013 reward discrepancy, exacerbating reward hacking. To address these limitations,
014 we propose **R2M** (**R**einforcement **R**eward **M**odel), a novel lightweight RLHF
015 framework. Specifically, we aim to go beyond vanilla reward models that solely
016 depend on the semantic representations of a pretrained LLM. Instead, we enhance
017 the reward model by incorporating the evolving hidden states of the policy (namely
018 **policy feedback**). We redesign the scoring head of the reward model to integrate
019 policy feedback and introduce a corresponding iterative lightweight training phase,
020 utilizing real-time policy feedback to enable adaption to policy distribution shifts.
021 Notably, without modifying the core RLHF algorithms, simply integrating R2M
022 enables the reward model to achieve iterative distribution alignment with accurate
023 reward allocation, yielding 4.8% to 5.6% win rate improvement on dialogue tasks
024 and 6.3% win rate improvement on document summarization tasks, while introduc-
025 ing marginal computational cost. This work points to a promising new direction
026 for improving the performance of reward models through real-time utilization of
027 feedback from policy models.

028 1 INTRODUCTION

029 Reinforcement Learning from Human Feedback (RLHF) has become a cornerstone technique for
030 aligning large language models (LLMs) with human values and preferences (Vemprala et al., 2023;
031 Shen & Zhang, 2024; Shen et al., 2025; Hu et al., 2024). However, RLHF faces a persistent challenge:
032 reward hacking. Instead of faithfully capturing human intent, policy models often exploit spurious
033 reward patterns, such as response length, markdown formatting, or superficial linguistic cues like
034 certain n-grams or emojis, to maximize rewards without genuinely improving alignment (Gao et al.,
035 2023; Coste et al., 2023; Eisenstein et al., 2023). The core issue lies in the reward model: trained on
036 limited preference data, it can only approximate human values. As the policy evolves during RLHF
037 training while the reward model remains fixed, distribution shift exacerbates approximation errors
038 (Wang et al., 2024b), ultimately leading to unreliable reward signals in optimization.

039 A natural solution is to iteratively update the reward model so that it adapts to the policy's evolving
040 behavior. Yet, direct retraining of the reward model at each iteration is computationally prohibitive.
041 To address this, one research direction emphasizes uncertainty-aware corrections. Coste et al.
042 (2023); Eisenstein et al. (2023); Zhai et al. (2023) penalize uncertain samples during policy training,
043 while Zhang et al. (2024a) introduce kernel-based uncertainty estimates derived from reward model
044 embeddings. Another line of work focuses on robust reward model retraining. Lang et al. (2024)
045 incorporate an unsupervised mutual information loss to counter distribution shift, and Liu et al. (2024)
046 augment training data by decomposing preferences relative to prompts. These methods trade off
047 efficiency and robustness, but leave open a critical question: Can we design a new RLHF framework
048 that preserves training efficiency while mitigating reward hacking effectively?

Our motivation stems from a key limitation of the standard RLHF pipeline: the unidirectional dependency between the policy and the reward model. While policies adapt to reward feedback, the reward model remains unaware of the policy's evolving internal states. This disconnect can allow policies to learn deceptive strategies, optimizing responses against a stale reward model rather than aligning with true human intent. To overcome this challenge, we propose **R2M** (**R**einforcement **R**eward **M**odel), a lightweight RLHF framework in which the reward model itself is reinforced iteratively by dynamically adapting to the policy's internal states, and it does not require any additional labeled data or environmental feedback to improve the performance.

Specifically, we observe that the hidden states of the policy encode latent patterns associated with reward hacking behaviors. Building on this insight, we aim to go beyond reward models that solely depend on the semantic representations of a pretrained LLM. Instead, we enhance the reward model by incorporating the evolving hidden states of the policy (namely **policy feedback**). To this end, we redesign the scoring head of the reward model so that it dynamically integrates these hidden states, enabling the reward model to adapt to distribution shifts in the policy. In our RLHF framework, this introduce a lightweight training component that learns to aggregate policy feedback directly, enhancing the reward model's representation without retraining the entire model. Owing to its efficiency, this mechanism can be seamlessly applied at every training round, ensuring continuous synchronization between the reward model and the policy.

The design of R2M offers two benefits: 1) **Iterative distribution alignment with accurate reward allocation.** The reward model integrates the policy's evolving hidden states which provide behaviorally grounded and semantically informed feedback. This mitigates distribution shifts, reduces reward hacking, and ensures more accurate reward assignment. 2) **Extremely lightweight overhead.** R2M only need to learn how to aggregate representations, introducing negligible additional cost.

Experimental results demonstrate that R2M significantly improves performance on dialogue tasks (trained on UltraFeedback (Cui et al., 2023), evaluated on Alpaca-Eval (Dubois et al., 2024)) and text summarization tasks (trained and evaluated on TL;DR summarization dataset). Specifically, R2M increases the AlpacaEval 2 win rate (WR) by 4.8% - 5.6%, the length-controlled win rate (LC) by 2.1% - 5.0% and the TL;DR win rate by 6.3% compared to baselines, while introducing only minimal computational cost. Furthermore, we conducted a comprehensive analysis, showing that R2M effectively strengthens the vanilla reward model and mitigates reward hacking with minimal additional training overhead.

2 PRELIMINARY

RLHF consists of three main steps: 1) Supervised Fine Tuning, 2) Reward Modeling, and 3) RL optimization, we provide a detailed workflow shown in Appendix G.1. As R2M is designed to directly integrated into the RL optimization phase, let us consider the following typical third-stage RL Optimization process:

First, in the **Trajectory Sampling** phase, at each training step $t \in [T]$, we update offline policy π_{old} to online policy π_θ . Then, given a query set $X_t = \{x_1, x_2, \dots, x_n\} \subset \mathcal{X}$, π_{old} is used to sample K responses $G_i = \{y_{i,j}\}_{j=1}^K$ for each $x_i \in X_t$.

Next is the **Reward Annotation** phase. Specifically, for each $(x_i, G_i), i \in [n]$, there are K query-response pairs $(x_i, y_{i,j}), j \in [K]$. We use a score-based reward model $r_\varphi(x, y)$ to assign rewards to each query-response pair (Ahmadian et al., 2024; Hu, 2025), obtaining $\{r_{i,j} | i \in [n], j \in [K]\}$, resulting in a batch $\mathcal{B} = \{(x_i, y_{i,j}, r_{i,j}) | i \in [n], j \in [K]\}$. After this process, we employ the RLOO approach (Ahmadian et al., 2024) to perform advantage estimation within each group G_i :

$$\hat{A}_{i,j} = r_{i,j} - \frac{1}{K-1} \sum_{\hat{j} \neq j} r_{i,\hat{j}}. \quad (1)$$

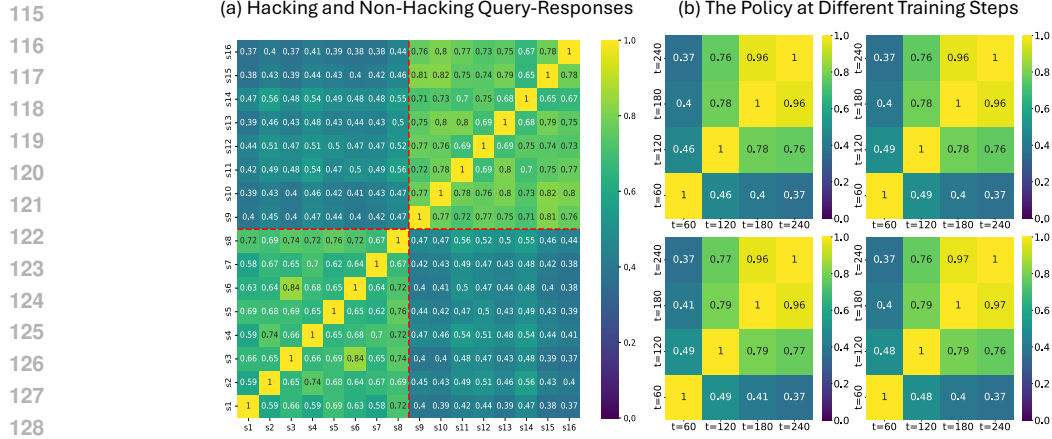
Finally, in the **Policy Optimization** phase, for each query-response pair $(x_i, y_{i,j})$, we perform a forward pass in the policy model π_θ and optimize π_θ using importance sampling by maximizing the following objective (Shao et al., 2024; Ahmadian et al., 2024), where ε and β are hyperparameters:

$$\left\{ \min \left[\frac{\pi_\theta(y_{i,j}|x_i, y_{i,j})}{\pi_{\theta_{old}}(y_{i,j}|x_i, y_{i,j})} \hat{A}_{i,j}, \text{clip} \left(\frac{\pi_\theta(y_{i,j}|x_i, y_{i,j})}{\pi_{\theta_{old}}(y_{i,j}|x_i, y_{i,j})}, 1 - \varepsilon, 1 + \varepsilon \right) \hat{A}_{i,j} \right] - \beta \mathbb{D}_{KL} [\pi_\theta \| \pi_{ref}] \right\}. \quad (2)$$

108 The design of R2M is based on the aforementioned RL optimization process. As a lightweight and
 109 significantly effective alternative, R2M can be seamlessly deployed to all REINFORCE-based RLHF
 110 frameworks. Due to resource constraints, we adopt RLOO as the primary baseline.
 111

112 3 MOTIVATION

114



130 **Figure 1: (a) Identification of Reward Hacking Patterns.** We show the similarity matrix of hidden
 131 states from forward passes of different query-response pairs for the same policy. The first 8 samples
 132 are sequences exhibiting reward hacking, while the last 8 are normal output responses. s denotes the
 133 query-response pairs. **(b) Policy Distribution Shift Analysis.** For a given query with four different
 134 responses, we display the similarity matrix of the policy across various training steps t .

135

136 We argue that hidden states in a transformer’s forward pass contain crucial information about a
 137 policy’s internal state and semantic information, making them effective for mitigating reward
 138 hacking. We validated this by computing hidden state similarity matrices. As shown in Figure 1 (a), responses
 139 with and without reward hacking show significant differences in their hidden state similarities.
 140 Figure 1 (b) shows that the same query-response’s hidden states from different training steps of a
 141 policy model are significantly different. Furthermore, as shown in Table 1, the average similarity
 142 between hacking and non-hacking responses is significantly lower than the similarity within each
 143 category. These findings strongly confirm that a policy’s hidden states offer valuable insights for
 144 detecting reward hacking.

144

145 To combat reward hacking, our R2M architecture decouples the issue from both the reward and
 146 policy models. We enhance the reward model’s alignment with true human preferences by leveraging
 147 policy feedback to improve reward allocation, moving beyond reliance on superficial patterns.
 148 Simultaneously, we tackle the policy model’s tendency to exploit fixed proxy rewards by enabling the
 149 reward model to dynamically adapt to the policy’s evolving internal state distribution, thus preventing
 150 the exploitation of fixed patterns.

150

151 Table 1: We report the average similarity of hidden states across three categories from multiple
 152 query-response pair groups, each group comprises 8 responses exhibiting reward hacking and 8
 153 normal responses.

154

Type	Hacking	Non-Hacking	Cross-Category
Avg-Sim	0.67	0.75	0.45

155

156 4 METHOD

157

158 Figure 2 illustrates the overall workflow of R2M. Built upon the RL optimization framework described
 159 in Section 2, R2M primarily consists of two key components: 1) how to structurally incorporate

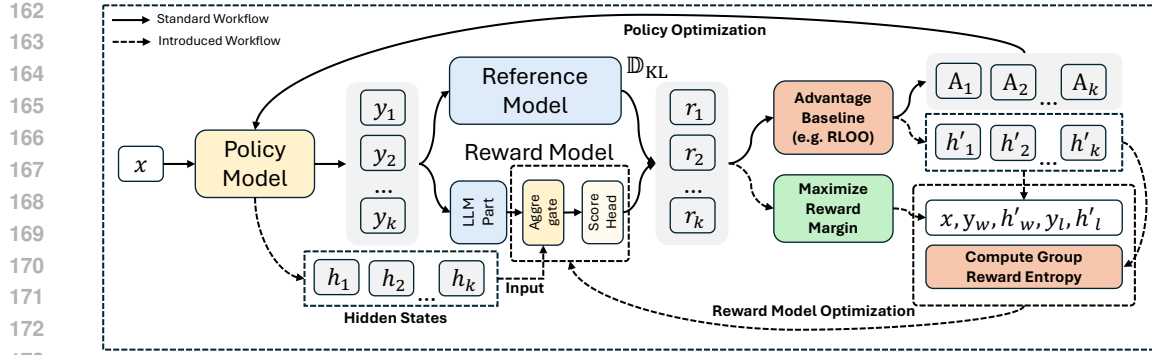


Figure 2: Overview of R2M. We first aggregate the last-layer hidden states from the policy h_i with the LLM part output of the reward model. This aggregated representation is then fed into the scoring head for reward prediction. When the policy updates, we get the real-time feedback h'_i and utilize it to construct preference pairs. Finally, we optimize the reward model by jointly minimizing the Bradley-Terry loss and the Group Reward Entropy.

feedback messages into the reward model (Section 4.1); 2) how to design the optimization objectives for the reward model (Section 4.2).

4.1 REWARD MODEL STRUCTURE

In this section, we focus on integrating the policy feedback from Section 2 into the reward model. As shown in Figure 3, we introduce a policy feedback data flow that bypasses the LLM part to directly enhance the original Reward Token Embedding (introduced in Appendix G.1). We formally redefine the reward model $r_\varphi(x, y)$ as **R2M** $r_\varphi(x, y, h)$. To effectively utilize the policy feedback, R2M contains two pivotal extra components: Sequence-to-Token Cross Attention and Time-Step-Based Weighted Combination.

Specifically, during the Trajectory Sampling phase, we collect the last-layer hidden states $h_{i,j} \in \mathbb{R}^{S_{i,j}-1 \times D_p}$ for each query-response pair $(x_i, y_{i,j}), i \in [n], j \in [K]$ from the policy. Here, $S_{i,j}$ denotes the effective length of the query-response pair, and D_p represents the hidden size of the policy. In the Reward Annotation phase, we first input $(x_i, y_{i,j}), i \in [n], j \in [K]$ into the LLM part of the reward model and obtain the Reward Token Embedding $H_{\text{last}}^{i,j} \in \mathbb{R}^{D_{\text{rm}}}$.

Sequence-to-Token Cross Attention. We introduce a cross-attention component to extract relevant information from hidden states of query-response pairs. Specifically, we inject policy feedback by performing a cross-attention operation from the sequence to a single token. This enables the query of the Reward Token Embedding $H_{\text{last}}^{i,j}$ to fully absorb the keys and values of the hidden state sequence $h_{i,j}$, which contains both policy state information and sequence semantic information, and updates it into a more information-rich Aggregated Reward Token Embedding $\hat{H}_{\text{last}}^{i,j}$.

Time-Step-Based Weighted Combination. After obtaining $\hat{H}_{\text{last}}^{i,j}$, we adopt an exploration-exploitation approach (Ban et al., 2021; 2024; Huang et al., 2025) to balance the weights of $H_{\text{last}}^{i,j}$ and $\hat{H}_{\text{last}}^{i,j}$, yielding the final Reward Token Embedding $H_{\text{fin}}^{i,j}$. Specifically, we use a time-step-based approach to gradually decrease the weight on the original Reward Token Embedding $H_{\text{last}}^{i,j}$ as follows:

$$H_{\text{fin}}^{i,j} = (1 - \omega(t))\hat{H}_{\text{last}}^{i,j} + \omega(t)H_{\text{last}}^{i,j}, \quad \omega(t) = \max\left(\frac{1}{2}\cos\left(\frac{t}{T}\pi\right) + \frac{1}{2}, \Omega\right), \quad (3)$$

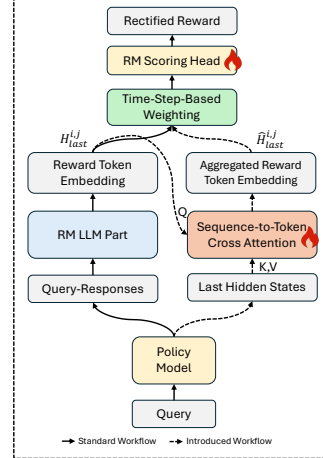


Figure 3: The structure of R2M. Building on the dataflow based on solely surface semantic information (left), R2M introduces an additional dataflow based on the policy feedback (right).

216 where t is the current training round, and T is the total number of training rounds. Ω is a hyperparameter
 217 used to ensure the minimum weight of the original Reward Token Embedding, and $\omega(t)$ is a
 218 monotonically decreasing function of t (Wu et al., 2025). When t is small, we prioritize leveraging
 219 the existing Reward Token Embedding $H_{\text{last}}^{i,j}$. As R2M iteratively updates during the training process
 220 (as discussed in Section 4.2), we gradually increase the influence of $\hat{H}_{\text{last}}^{i,j}$ to enable the reward model
 221 to progressively identify and adapt to the distribution shift of the policy. As a result of balancing the
 222 exploitation of the original embedding with the exploration of policy feedback information, $H_{\text{fin}}^{i,j}$ is
 223 then mapped by the reward head ϕ to the final scalar reward $r_\varphi(x_i, y_{i,j}, h_{i,j}) = \phi(H_{\text{fin}}^{i,j}) \in \mathbb{R}$.
 224

225 4.2 ITERATIVE REWARD MODEL LIGHTWEIGHT OPTIMIZATION

227 In Section 4.1, we have introduced policy feedback into the reward model. However, the semantic
 228 spaces are not yet aligned, making it challenging for the reward model to directly utilize this
 229 information. To address this, we incorporate an extra lightweight Reward Model Optimization phase
 230 following the Policy Optimization phase at each training step, and propose a novel optimization
 231 objective for R2M, namely the Group Reward Entropy Bradley-Terry loss.

232 **Hidden State Update.** To ensure that the hidden states $h_{i,j}$ remain up-to-date and accurately
 233 reflect the internal states of the policy π_θ , we update $h_{i,j}$ whenever $(x_i, y_{i,j})$ is used to update π_θ .
 234 Specifically, during the forward pass of π_θ on $(x_i, y_{i,j})$, we fetch the latest hidden states $h_{i,j}$, which
 235 incurs no additional computational overhead. Since the policy model is trained for k epochs on the
 236 same batch at each training step t (Shao et al., 2024; Hu, 2025), this update is performed only in the
 237 final epoch. For notational simplicity, we continue to use $h_{i,j}$ to denote the most recent hidden states.
 238 This mechanism enables the reward model to dynamically capture distribution shifts in real time as
 239 the policy evolves.

240 **Group Reward Entropy Bradley-Terry Loss.** To enhance the robustness of the reward model
 241 by incorporating policy feedback during score allocation, we propose the Group Reward Entropy
 242 Bradley-Terry Loss. For each query-response group (x_i, G_i) , to ensure the reliability of preference
 243 labels, we select only the samples with the highest and lowest scores to construct the preference
 244 pair, resulting in $\{x_i, y_{i,w}, h_{i,w}, y_{i,l}, h_{i,l}\}$. Then, we can establish the Bradley-Terry optimization
 245 objective as:

$$246 \quad \mathcal{L}_{\text{BT}}(i : \varphi) = -\log \sigma(r_\varphi(x_i, y_{i,w}, h_{i,w}) - r_\varphi(x_i, y_{i,l}, h_{i,l})), \quad (4)$$

247 which allows the reward model to be continuously optimized as the policy evolves.

248 However, in practice, the reward model often assigns nearly identical scores to responses within a
 249 group, especially in the later phases of RL optimization when the responses become more ho-
 250 mogeneous. To address this issue, we introduce an entropy regularization term to encourage
 251 greater reward diversity within each group. Specifically, for each group (x_i, G_i) , we first com-
 252 pute the foward pass of the reward model φ on all samples to get newly allocated reward scores
 253 $r_{i,j} = r_\varphi(x_i, y_{i,j}, h_{i,j}), j \in [K]$. We define the Group Reward Entropy for group (x_i, G_i) as

$$254 \quad H_{\text{group}}^i = -\sum_{j=1}^K p_{i,j} \log p_{i,j}, \quad \text{where } p_{i,j} = \text{softmax}\left(\frac{r_{i,j} - \text{mean}(\mathbf{r})}{\text{std}(\mathbf{r})}\right), \quad (5)$$

255 where $\mathbf{r} = \{r_{i,1}, r_{i,2}, \dots, r_{i,K}\}$, and i is the group index, the softmax operation is applied across
 256 all standardized reward values within the group to get the relative preference of each sample. By
 257 minimizing the GRE, we sharpen the distribution $p_{i,j}$, thereby amplifying the score disparities within
 258 the group. Finally, the overall optimization objective of R2M is given by:

$$259 \quad \mathcal{L}_{\text{FIN}}(i : \varphi) = (1 - \alpha)\mathcal{L}_{\text{BT}}(i : \varphi) + \alpha H_{\text{group}}^i, \quad (6)$$

260 where α is a tunable hyperparameter. Through this optimization objective, we enable the reward model
 261 to progressively learn to provide reasonable and more confident reward signals while incorporating
 262 real-time policy feedback, thereby allowing it to automatically adapt to the policy’s distribution shifts.

263 **Workflow.** Algorithm 1 illustrates the workflow of our proposed R2M algorithm, The modifications
 264 primarily involve utilizing both shallow semantic information $(x_i, y_{i,j})$ and policy feedback $h_{i,j}$
 265 during the Reward Annotation phase, as well as introducing an additional lightweight Reward Model
 266 Optimization phase to iteratively update the reward model based on real-time policy feedback.

270 *Policy Optimization (Lines 2-14).* We retain the same Policy Optimization phase as described in
 271 Section 2, with the only difference being that we update the policy feedback for each query-response
 272 pair using the real-time updated π_θ as mentioned in Section 4.2.
 273

274 *Reward Model Optimization (Lines 15-20).* To preserve the general representational capacity of the
 275 reward model’s LLM part while enhancing the relatively weaker linear projection component, we
 276 solely update the cross-attention component and the scoring head ϕ , leaving the LLM part frozen.
 277 We provide detailed design motivations in the Appendix G.2. This approach significantly reduces the
 278 overall computational cost of R2M, ensuring the feasibility of iteratively updating the reward model.
 279

Algorithm 1 Proposed RLHF Framework: R2M

280 **Require:** Initial policy model $\pi_\theta \leftarrow \pi_{\text{SFT}}$, reference model π_{ref} , reward model r_φ , queries \mathcal{X}
 281 1: **for** step = 1, ..., T **do**
 282 2: Sample a batch $\mathcal{X}_{\text{batch}} = \{x_i\}, i \in [n]$ from \mathcal{X}
 283 3: Update the old policy model $\pi_{\text{old}} \leftarrow \pi_\theta$
 284 4: **Trajectory Sampling:**
 285 5: Sample a group of output $G_i = \{y_{i,j}\}, j \in [K] \sim \pi_{\text{old}}(\cdot | x_i)$ for each query $x_i \in \mathcal{X}_{\text{batch}}$
 286 6: Get the last-layer hidden states $\{h_{i,j}\}, j \in [K]$ from π_{old}
 287 7: **Reward Annotation:**
 288 8: Compute the rewards with policy feedback $\{r_\varphi(x_i, y_{i,j}, h_{i,j})\}, i \in [n], j \in [K]$
 289 9: Compute $\{\hat{A}_{i,j}\}, j \in [K]$ within each G_i for query x_i through Equation 1
 290 10: **Policy Optimization:**
 291 11: **for** iteration = 1, ..., k **do**
 292 12: Update the policy model π_θ by maximizing the RLOO objective through Equation 2
 293 13: Update $h_{i,j}, i \in [n], j \in [K]$ from the policy forward when iteration = k
 294 14: **end for**
 295 15: **Reward Model Optimization:**
 296 16: Get preference pair $\{x_i, y_{i,w}, h_{i,w}, y_{i,l}, h_{i,l}\}$ according to Section 4.2 within each G_i
 297 17: Compute $\mathcal{L}_{\text{BT}}(i : \varphi)$ according to Equation 4
 298 18: Compute $\{r_\varphi(x_i, y_{i,j}, h_{i,j})\}, j \in [K]$ within each G_i
 299 19: Compute Group Reward Entropy H_{group}^i according to Equation 5
 300 20: Update reward model r_φ according to Equation 6
 301 21: **end for**
 302 **Ensure:** π_θ, r_φ

 303
 304 **5 EXPERIMENT**

305
 306 In this section, we present the primary experimental results along with their analysis. We set the
 307 learning rate of R2M to 1×10^{-6} , the weight coefficient of the hybrid loss $\alpha = 0.5$, and the width of
 308 cross-attention component to 2048. during the entire training process, we sample 12k trajectories
 309 with a maximum length of 512 for the dialogue task, and 1000k trajectories with a maximum length
 310 of 50 for the document summarization task. Additional implementation details of R2M are provided
 311 in Appendix F due to space constraints.
 312

 313 **5.1 MAIN EXPERIMENT RESULTS**

314 In this section, we present the experimental results of R2M on dialogue and document summarization
 315 tasks. We integrated R2M into RLOO and compare it against state-of-the-art REINFORCE-based
 316 RLHF algorithms.
 317

318 For dialogue task, We considered the current mainstream evaluation frameworks, utilizing queries
 319 from UltraFeedback (Cui et al., 2023) for online RL optimization and conducting evaluations with
 320 AlpacaEval 2 (Dubois et al., 2024), which is a widely used chat-based evaluation benchmark. Detailed
 321 experimental settings can be found in Appendix F.2.

322 Next, we considered a classic RLHF task, summarization: x is a forum post from Reddit, and the
 323 policy must generate a summary y of the main points in the post. The corresponding experimental
 324 settings are detailed in Appendix F.3.

(1) **R2M consistently achieves superior performance.** As shown in Table 2, the incorporation of policy feedback and iterative updates of the reward model enable R2M to achieve the highest scores across all evaluation metrics. Specifically, R2M outperforms the best-performing baseline by margins ranging from 2.1% to 5.0% on the AlpacaEval 2 LC win rate, from 4.8% to 5.6% on the AlpacaEval 2 win rate and 6.3% on the TL;DR win rate. These results underscore the broad applicability of R2M in preference optimization and its effectiveness in aligning large language models with human preferences.

(2) **R2M significantly enhances the reward model.** The sole difference between R2M and RLOO is the replacement of a frozen reward model with one iteratively updated and allocating rewards via policy feedback. Compared to RLOO, R2M achieved a 2.9% to 6.1% increase in LC win rate, a 5.2% to 8.0% increase in raw win rate, and a 6.3% increase in TL;DR win rate. Notably, the LC win rate improvement was accomplished while reducing average sequence length to a certain extent. These substantial improvements are entirely due to the stronger reward model of R2M. This clearly demonstrate the effectiveness of R2M’s integration of feedback to iteratively enhance the reward model. This enhancement can be attributed to two factors: real-time alignment with the policy model and additionally introduced deep semantic understanding, thanks to the rich information from policy feedback discussed in Section 3.

Table 2: Results of R2M compared with baselines across different experimental settings. LC and WR denote length-controlled and raw win rate, respectively. Here, **bold** denotes the best performance, underline indicates the second-best performance.

Method	Dialogue						Summarization	
	Qwen2.5-3B-Instruct			LLaMA3-8B-Instruct				
	LC(%)	WR(%)	Avg Len	LC(%)	WR(%)	Avg Len		
SFT	15.5	15.8	2218	22.9	22.6	1899	42.3	
GRPO	<u>22.7</u>	25.6	3012	<u>29.5</u>	<u>32.6</u>	2216	75.2	
ReMax	21.8	25.1	2916	28.7	30.7	2289	75.1	
REINFORCE++	21.4	<u>26.4</u>	3252	29.3	31.8	2192	74.3	
RLOO	21.9	26.0	3174	28.4	30.2	2186	<u>75.3</u>	
R2M	24.8	31.2	2911	34.5	38.2	2011	81.6	

5.2 ANALYSIS

In this section, we present additional analytical experiments to clarify, from a principled perspective, the reasons behind R2M’s effectiveness in RL optimization.

R2M maintains reward consistency while allocating higher rewards.

We compared the average R2M rewards to that annotated by the vanilla reward model during RL optimization process. Specifically, every 5 training steps, we sampled 128 queries from the test set as a batch, prompted the policy π_θ to generate complete responses, and scored them using the reward model. We report the average scores for each batch. As shown in Figure 4, **Reward without Feedback** is provided by a frozen reference reward model, while **Reward with Feedback** corresponds to R2M. To rigorously compare the effect of policy feedback, we include an additional control group **Reward with Noise**, where we replace the feedback with Gaussian noise. we first observe that R2M exhibits a consistent reward trend compared to the reference reward model, directly indicating that R2M can reliably provide reasonable rewards. Additionally, R2M consistently allocating higher rewards. In contrast, when noise with the same mean and standard deviation is introduced, the resulting reward signals are significantly reduced. This clearly suggests that policy feedback contains beneficial information, consistent with the phenomena observed in Section 3. We hypothesize that the higher

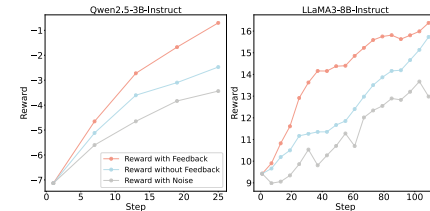
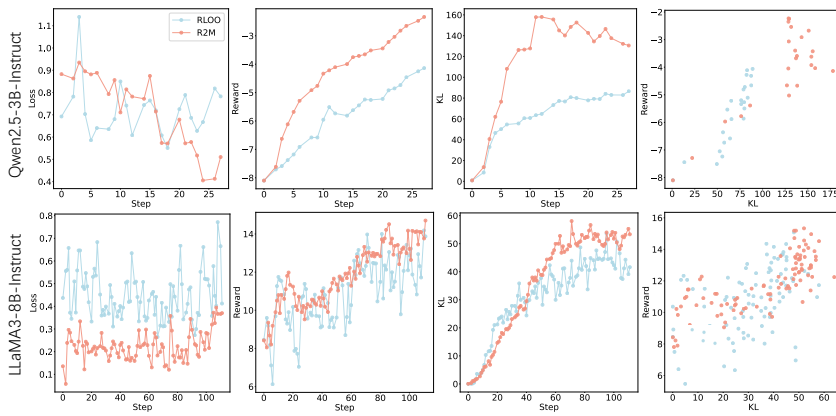


Figure 4: Comparison of average rewards under various conditions.

378 average reward allocation results from the GRE minimization objective of R2M, which encourages
 379 the reward model to assign higher reward values to high-quality responses with greater confidence.
 380

381 **R2M encourages substantial and effective policy updates.** Figure 5 illustrates the performance
 382 curves of R2M compared with RLOO during RL optimization for dialogue tasks. As shown in the left
 383 two columns, R2M demonstrates a significantly higher reward curve and lower loss curve compared
 384 to RLOO. Generally, this indicates more effective training outcomes. From the perspective of KL
 385 divergence, R2M encourages larger parameter shifts in the model to achieve greater rewards. As
 386 shown in the right two columns of Figure 5, R2M exhibits a greater policy distribution shift in the
 387 KL-Step curve and a denser distribution in the high-reward, high-KL region of the Reward-KL scatter
 388 plot. Aggressive policy updates readily lead to reward hacking (Coste et al., 2023), whereas R2M,
 389 compared to RLOO, achieves substantial performance gains demonstrated in Section 5.1, rather than
 390 causing training collapse. This indicates that R2M effectively improves the reward model’s resistance
 391 to policy’s exploitation of specific patterns, enabling more aggressive policy updates in the correct
 392 direction without triggering reward hacking.



407 Figure 5: We compare RLOO and R2M in terms of loss, reward and KL divergence during RL
 408 optimization, using Qwen2.5-3B-Instruct and LLaMA3-8B-Instruct as policy models, and Skywork-
 409 Reward-V2-Llama-3.1-8B as the reward model. For KL divergence, we calculate it as the average of
 410 log probability differences between the reference model and the policy model for each token.

412 **R2M significantly improves the accuracy of the reward model.** We compare the accuracy of
 413 R2M and the vanilla reward model on the test set of UltraFeedback before and after running the R2M
 414 pipeline, as experimental details shown in Appendix F.4. As shown in Table 3, after iterative updates,
 415 R2M achieves accuracy improvements of 5.1% and 6.3% compared to the original reward model.
 416 These results indicate that R2M significantly enhances the accuracy of the reward model, which is
 417 crucial for preventing reward hacking and improving training effect (Rafailov et al., 2023; Lambert
 418 et al., 2024; Adler et al., 2024). Before training, incorporating policy feedback results in accuracy
 419 decreases of 4.0% and 3.1%. This clearly demonstrates that policy feedback cannot be used directly,
 420 highlighting the effectiveness and necessity of the Reward Model Optimization phase in R2M.

422 Table 3: Comparison of the accuracy of reward models under different
 423 conditions. "Without Feedback" refers to the frozen reference reward
 424 model, while "With Feedback" represents R2M before and after the
 425 R2M pipeline.

427 Reward Model Type	428 Policy Model Type	
	429 Qwen2.5(%)	430 LLaMA3(%)
431 without Feedback	72.3	72.3
432 with Feedback (Before-Training)	68.3	69.2
433 with Feedback (After-Training)	77.4	78.6

426
Table 4: The TL;DR Re-
 427 sult of R2M Compared
 428 with Baselines.

429 Method	430 WR(%)
431 SFT	33.7
432 RLOO	8.7
433 R2M	61.6

432 **R2M can strongly mitigate reward hacking.** In this section, we present a case study demonstrating
 433 that R2M not only largely enhances the robustness and performance of RL optimization, but also
 434 effectively prevents training collapse due to reward hacking. Specifically, when performing RL
 435 optimization with RLOO on the TL;DR task using Pythia-1B-TL;DR-SFT and Pythia-1B-TL;DR-
 436 RM, we observed that the trained model produced completions without spaces, despite maintaining
 437 correct semantic meaning. This issue arises because the Pythia tokenizer controls the presence of
 438 spaces through special token prefixes, and the reward model exhibits a erroneous preference for
 439 token sequences without spaces. After applying R2M, this severe reward hacking phenomenon was
 440 eliminated, and a stable improvement in win rate was achieved after RL optimization, as shown in
 441 Table 4. These results indicate that R2M can effectively mitigate reward hacking, even in cases of
 442 complete training collapse, under identical hyperparameter settings. Detailed experimental results are
 443 provided in Appendix F.5.

444 5.3 COMPUTATIONAL COST ANALYSIS

446 R2M is lightweight and compute-efficient. Figure 6 il-
 447 lustrates the peak single-GPU memory usage and over-
 448 all runtime of R2M compared to RLOO under setting of
 449 LLaMA environment. R2M introduces negligible addi-
 450 tional overheads compared to the performance gains it
 451 achieves. This can attribute to two main factors. First,
 452 policy feedback can be directly obtained and its aggrega-
 453 tion solely involves lightweight attention computations.
 454 Second, R2M does not update the reward model’s LLM
 455 part, and its cross-attention module and scoring head are
 456 relatively lightweight.

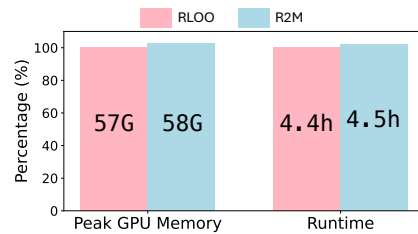
457 **For the ablation study, refer to Appendix E.**

459 6 RELATED WORKS

461 **REINFORCE-based RLHF Algorithms.** RLHF is a critical technique for aligning large language
 462 models with human preferences (Ouyang et al., 2022; Bai et al., 2022a). The classical RLHF
 463 pipeline typically comprises three phases: supervised fine-tuning (Geng et al., 2023), reward model
 464 training (Gao et al., 2023), and policy optimization against the reward model (Schulman et al., 2017).
 465 As a classic reinforcement learning algorithm, Proximal Policy Optimization (PPO) (Schulman et al.,
 466 2017) is widely used in the third stage of RLHF. Recently, many researchers have proposed a series
 467 of REINFORCE-based methods, such as ReMax (Li et al., 2023), RLOO (Ahmadian et al., 2024),
 468 GRPO (Shao et al., 2024) and REINFORCE++ (Hu, 2025) to avoid the computational overhead
 469 associated with the critic model while still obtaining relatively accurate sequence-wise advantage
 470 estimations. These methods design alternative techniques to calculate the baseline reward for each
 471 prompt as the advantage estimation.

472 7 CONCLUSION

475 To mitigate reward hacking exacerbated by policy’s distribution shifts, we propose **R2M**, a novel
 476 lightweight RLHF framework. By incorporating the policy’s evolving hidden states, R2M enhances
 477 the reward model’s accuracy while maintaining robustness against reward hacking. Without modi-
 478 fying current RLHF algorithms, Simply integrating R2M into the framework achieves significant
 479 performance improvements while introducing only marginal additional computational costs.



474 Figure 6: Computational cost comparison
 475 between RLOO and R2M: similar
 476 runtime and GPU memory usage.

486 REFERENCES
487

488 Bo Adler, Niket Agarwal, Ashwath Aithal, Dong H Anh, Pallab Bhattacharya, Annika Brundyn,
489 Jared Casper, Bryan Catanzaro, Sharon Clay, Jonathan Cohen, et al. Nemotron-4 340b technical
490 report. *arXiv preprint arXiv:2406.11704*, 2024.

491 Arash Ahmadian, Chris Cremer, Matthias Gallé, Marzieh Fadaee, Julia Kreutzer, Olivier Pietquin,
492 Ahmet Üstün, and Sara Hooker. Back to basics: Revisiting reinforce style optimization for learning
493 from human feedback in llms. *arXiv preprint arXiv:2402.14740*, 2024.

494 AI@Meta. Llama 3 model card. 2024. URL [https://github.com/meta-llama/llama3/
495 blob/main/MODEL_CARD.md](https://github.com/meta-llama/llama3/blob/main/MODEL_CARD.md).

496 Yuntao Bai, Andy Jones, Kamal Ndousse, Amanda Askell, Anna Chen, Nova DasSarma, Dawn Drain,
497 Stanislav Fort, Deep Ganguli, Tom Henighan, et al. Training a helpful and harmless assistant with
498 reinforcement learning from human feedback. *arXiv preprint arXiv:2204.05862*, 2022a.

499 Yuntao Bai, Saurav Kadavath, Sandipan Kundu, Amanda Askell, Jackson Kernion, Andy Jones,
500 Anna Chen, Anna Goldie, Azalia Mirhoseini, Cameron McKinnon, Carol Chen, Catherine Olsson,
501 Christopher Olah, Danny Hernandez, Dawn Drain, Deep Ganguli, Dustin Li, Eli Tran-Johnson,
502 Ethan Perez, Jamie Kerr, Jared Mueller, Jeffrey Ladish, Joshua Landau, Kamal Ndousse, Kamile
503 Lukosuite, Liane Lovitt, Michael Sellitto, Nelson Elhage, Nicholas Schiefer, Noemi Mercado,
504 Nova DasSarma, Robert Lasenby, Robin Larson, Sam Ringer, Scott Johnston, Shauna Kravec,
505 Sheer El Showk, Stanislav Fort, Tamera Lanham, Timothy Telleen-Lawton, Tom Conerly, Tom
506 Henighan, Tristan Hume, Samuel R. Bowman, Zac Hatfield-Dodds, Ben Mann, Dario Amodei,
507 Nicholas Joseph, Sam McCandlish, Tom Brown, and Jared Kaplan. Constitutional ai: Harmlessness
508 from ai feedback, 2022b. URL <https://arxiv.org/abs/2212.08073>.

509 Yikun Ban, Yuchen Yan, Arindam Banerjee, and Jingrui He. Ee-net: Exploitation-exploration neural
510 networks in contextual bandits. *arXiv preprint arXiv:2110.03177*, 2021.

511 Yikun Ban, Ishika Agarwal, Ziwei Wu, Yada Zhu, Kommy Weldemariam, Hanghang Tong, and
512 Jingrui He. Neural active learning beyond bandits. *arXiv preprint arXiv:2404.12522*, 2024.

513 Ralph Allan Bradley and Milton E Terry. Rank analysis of incomplete block designs: I. the method
514 of paired comparisons. *Biometrika*, 39(3/4):324–345, 1952.

515 Tom Brown, Benjamin Mann, Nick Ryder, Melanie Subbiah, Jared D Kaplan, Prafulla Dhariwal,
516 Arvind Neelakantan, Pranav Shyam, Girish Sastry, Amanda Askell, et al. Language models are
517 few-shot learners. *Advances in neural information processing systems*, 33:1877–1901, 2020.

518 Junhao Chen, Shengding Hu, Zhiyuan Liu, and Maosong Sun. States hidden in hidden states: Llms
519 emerge discrete state representations implicitly. *arXiv preprint arXiv:2407.11421*, 2024.

520 Lichang Chen, Chen Zhu, Juhai Chen, Davit Soselia, Tianyi Zhou, Tom Goldstein, Heng Huang,
521 Mohammad Shoeybi, and Bryan Catanzaro. Odin: Disentangled reward mitigates hacking in rlhf.
522 In *Forty-first International Conference on Machine Learning*.

523 Ting Chen, Simon Kornblith, Mohammad Norouzi, and Geoffrey Hinton. A simple framework for
524 contrastive learning of visual representations. *arXiv preprint arXiv:2002.05709*, 2020.

525 Thomas Coste, Usman Anwar, Robert Kirk, and David Krueger. Reward model ensembles help
526 mitigate overoptimization. *arXiv preprint arXiv:2310.02743*, 2023.

527 Ganqu Cui, Lifan Yuan, Ning Ding, Guanming Yao, Wei Zhu, Yuan Ni, Guotong Xie, Zhiyuan Liu,
528 and Maosong Sun. Ultrafeedback: Boosting language models with high-quality feedback. 2023.

529 Carson Denison, Monte MacDiarmid, Fazl Barez, David Duvenaud, Shauna Kravec, Samuel Marks,
530 Nicholas Schiefer, Ryan Soklaski, Alex Tamkin, Jared Kaplan, Buck Shlegeris, Samuel R. Bowman,
531 Ethan Perez, and Evan Hubinger. Sycophancy to subterfuge: Investigating reward-tampering in
532 large language models, 2024. URL <https://arxiv.org/abs/2406.10162>.

533 Yann Dubois, Balázs Galambosi, Percy Liang, and Tatsunori B Hashimoto. Length-controlled
534 alpacaeval: A simple way to debias automatic evaluators. *arXiv preprint arXiv:2404.04475*, 2024.

540 Jacob Eisenstein, Chirag Nagpal, Alekh Agarwal, Ahmad Beirami, Alex D’Amour, DJ Dvijotham,
 541 Adam Fisch, Katherine Heller, Stephen Pfohl, Deepak Ramachandran, et al. Helping or herd-
 542 ing? reward model ensembles mitigate but do not eliminate reward hacking. *arXiv preprint*
 543 *arXiv:2312.09244*, 2023.

544 Leo Gao, John Schulman, and Jacob Hilton. Scaling laws for reward model overoptimization. In
 545 *International Conference on Machine Learning*, pp. 10835–10866. PMLR, 2023.

546 Xinyang Geng, Arnav Gudibande, Hao Liu, Eric Wallace, Pieter Abbeel, Sergey Levine, and Dawn
 547 Song. Koala: A dialogue model for academic research. *Blog post, April*, 1:6, 2023.

548 Wei Guo, Siyuan Lu, Yiqi Tong, Zhaojun Hu, Fuzhen Zhuang, Xiao Zhang, Tao Fan, and Jin
 549 Dong. H2tune: Federated foundation model fine-tuning with hybrid heterogeneity. *arXiv preprint*
 550 *arXiv:2507.22633*, 2025.

551 Jian Hu. Reinforce++: A simple and efficient approach for aligning large language models. *arXiv*
 552 *preprint arXiv:2501.03262*, 2025.

553 Jian Hu, Xibin Wu, Zilin Zhu, Weixun Wang, Dehao Zhang, Yu Cao, et al. Openrlhf: An easy-to-use,
 554 scalable and high-performance rlhf framework. *arXiv preprint arXiv:2405.11143*, 2024.

555 Zixuan Huang, Yikun Ban, Lean Fu, Xiaojie Li, Zhongxiang Dai, Jianxin Li, and Deqing Wang.
 556 Adaptive sample scheduling for direct preference optimization. *arXiv preprint arXiv:2506.17252*,
 557 2025.

558 Polina Kirichenko, Pavel Izmailov, and Andrew Gordon Wilson. Last layer re-training is sufficient
 559 for robustness to spurious correlations. *arXiv preprint arXiv:2204.02937*, 2022.

560 Tyler Labonte and Vidya Muthukumar. Towards last-layer retraining for group
 561 robustness with fewer annotations. <https://synthical.com/article/f641541d-124b-4974-9a73-d29f3f98c0b8>, 8 2023.

562 Nathan Lambert, Valentina Pyatkin, Jacob Morrison, LJ Miranda, Bill Yuchen Lin, Khyathi Chandu,
 563 Nouha Dziri, Sachin Kumar, Tom Zick, Yejin Choi, et al. Rewardbench: Evaluating reward models
 564 for language modeling. *arXiv preprint arXiv:2403.13787*, 2024.

565 Hao Lang, Fei Huang, and Yongbin Li. Fine-tuning language models with reward learning on policy.
 566 *arXiv preprint arXiv:2403.19279*, 2024.

567 Yoonho Lee, Annie S. Chen, Fahim Tajwar, Ananya Kumar, Huaxiu Yao, Percy Liang, and Chelsea
 568 Finn. Surgical fine-tuning improves adaptation to distribution shifts, 2023.

569 Ziniu Li, Tian Xu, Yushun Zhang, Zhihang Lin, Yang Yu, Ruoyu Sun, and Zhi-Quan Luo. Remax: A
 570 simple, effective, and efficient reinforcement learning method for aligning large language models.
 571 *arXiv preprint arXiv:2310.10505*, 2023.

572 Chris Yuhao Liu, Liang Zeng, Yuzhen Xiao, Jujie He, Jiacao Liu, Chaojie Wang, Rui Yan, Wei Shen,
 573 Fuxiang Zhang, Jiacheng Xu, Yang Liu, and Yahui Zhou. Skywork-reward-v2: Scaling preference
 574 data curation via human-ai synergy. *arXiv preprint arXiv:2507.01352*, 2025.

575 Tianqi Liu, Wei Xiong, Jie Ren, Lichang Chen, Junru Wu, Rishabh Joshi, Yang Gao, Jiaming Shen,
 576 Zhen Qin, Tianhe Yu, et al. Rrm: Robust reward model training mitigates reward hacking. *arXiv*
 577 *preprint arXiv:2409.13156*, 2024.

578 Xiaodong Lu, Mingzhe Liu, Tongyu Zhu, Leilei Sun, Jibin Wang, Weifeng Lv, Yikun Ban, and Deqing
 579 Wang. Adaptive sampling-based dynamic graph learning for information diffusion prediction.
 580 *ACM Trans. Inf. Syst.*, 43(5), August 2025. ISSN 1046-8188. doi: 10.1145/3744643. URL
 581 <https://doi.org/10.1145/3744643>.

582 Bonan Min, Hayley Ross, Elior Sulem, Amir Pouran Ben Veyseh, Thien Huu Nguyen, Oscar Sainz,
 583 Eneko Agirre, Ilana Heintz, and Dan Roth. Recent advances in natural language processing via
 584 large pre-trained language models: A survey. *ACM Computing Surveys*, 56(2):1–40, 2023.

594 Long Ouyang, Jeff Wu, Xu Jiang, Diogo Almeida, Carroll L. Wainwright, Pamela Mishkin, Chong
 595 Zhang, Sandhini Agarwal, Katarina Slama, Alex Ray, John Schulman, Jacob Hilton, Fraser Kelton,
 596 Luke E. Miller, Maddie Simens, Amanda Askell, Peter Welinder, Paul Francis Christiano, Jan
 597 Leike, and Ryan J. Lowe. Training language models to follow instructions with human feedback.
 598 In *NeurIPS*, 2022.

599 Rafael Rafailov, Archit Sharma, Eric Mitchell, Christopher D Manning, Stefano Ermon, and Chelsea
 600 Finn. Direct preference optimization: Your language model is secretly a reward model. In
 601 *Thirty-seventh Conference on Neural Information Processing Systems*, 2023. URL <https://arxiv.org/abs/2305.18290>.

602
 603 Alexandre Ramé, Johan Ferret, Nino Vieillard, Robert Dadashi, Léonard Hussenot, Pierre-Louis
 604 Cedoz, Pier Giuseppe Sessa, Sertan Girgin, Arthur Douillard, and Olivier Bachem. Warp: On
 605 the benefits of weight averaged rewarded policies, 2024a. URL <https://arxiv.org/abs/2406.16768>.

606 Alexandre Ramé, Nino Vieillard, Léonard Hussenot, Robert Dadashi, Geoffrey Cideron, Olivier
 607 Bachem, and Johan Ferret. Warm: On the benefits of weight averaged reward models, 2024b. URL
 608 <https://arxiv.org/abs/2401.12187>.

609
 610 Carlos Riquelme, George Tucker, and Jasper Snoek. Deep bayesian bandits showdown: An empirical
 611 comparison of bayesian deep networks for thompson sampling, 2018.

612 John Schulman, Filip Wolski, Prafulla Dhariwal, Alec Radford, and Oleg Klimov. Proximal policy
 613 optimization algorithms, 2017.

614 Zhihong Shao, Peiyi Wang, Qihao Zhu, Runxin Xu, Junxiao Song, Xiao Bi, Haowei Zhang,
 615 Mingchuan Zhang, YK Li, Yang Wu, et al. Deepseekmath: Pushing the limits of mathematical
 616 reasoning in open language models. *arXiv preprint arXiv:2402.03300*, 2024.

617 Wei Shen and Chuheng Zhang. Policy filtration in rlhf to fine-tune llm for code generation. *arXiv
 618 preprint arXiv:2409.06957*, 2024.

619 Wei Shen, Guanlin Liu, Zheng Wu, Ruofei Zhu, Qingping Yang, Chao Xin, Yu Yue, and Lin Yan.
 620 Exploring data scaling trends and effects in reinforcement learning from human feedback. *arXiv
 621 preprint arXiv:2503.22230*, 2025.

622 Prasann Singhal, Tanya Goyal, Jiacheng Xu, and Greg Durrett. A long way to go: Investigating
 623 length correlations in rlhf. *arXiv preprint arXiv:2310.03716*, 2023.

624 Qwen Team. Qwen2.5: A party of foundation models, September 2024. URL <https://qwenlm.github.io/blog/qwen2.5/>.

625 Ashish Vaswani, Noam Shazeer, Niki Parmar, Jakob Uszkoreit, Llion Jones, Aidan N Gomez, Łukasz
 626 Kaiser, and Illia Polosukhin. Attention is all you need. *Advances in neural information processing
 627 systems*, 30, 2017.

628 Sai Vemprala, Rogerio Bonatti, Arthur Bucker, and Ashish Kapoor. Chatgpt for robotics: Design
 629 principles and model abilities. *Microsoft Auton. Syst. Robot. Res*, 2:20, 2023.

630 Binghai Wang, Rui Zheng, Lu Chen, Yan Liu, Shihan Dou, Caishuang Huang, Wei Shen, Senjie Jin,
 631 Enyu Zhou, Chenyu Shi, Songyang Gao, Nuo Xu, Yuhao Zhou, Xiaoran Fan, Zhiheng Xi, Jun
 632 Zhao, Xiao Wang, Tao Ji, Hang Yan, Lixing Shen, Zhan Chen, Tao Gui, Qi Zhang, Xipeng Qiu,
 633 Xuanjing Huang, Zuxuan Wu, and Yu-Gang Jiang. Secrets of rlhf in large language models part ii:
 634 Reward modeling, 2024a. URL <https://arxiv.org/abs/2401.06080>.

635 Binghai Wang, Rui Zheng, Lu Chen, Yan Liu, Shihan Dou, Caishuang Huang, Wei Shen, Senjie Jin,
 636 Enyu Zhou, Chenyu Shi, et al. Secrets of rlhf in large language models part ii: Reward modeling.
 637 *arXiv preprint arXiv:2401.06080*, 2024b.

638 Jason Wei, Yi Tay, Rishi Bommasani, Colin Raffel, Barret Zoph, Sebastian Borgeaud, Dani Yogatama,
 639 Maarten Bosma, Denny Zhou, Donald Metzler, et al. Emergent abilities of large language models.
 640 *arXiv preprint arXiv:2206.07682*, 2022.

648 Siye Wu, Jian Xie, Yikai Zhang, Aili Chen, Kai Zhang, Yu Su, and Yanghua Xiao. Arm: Adaptive
 649 reasoning model. *arXiv preprint arXiv:2505.20258*, 2025.
 650

651 Hongyan Xie, Yitong Yao, Yikun Ban, Zixuan Huang, Deqing Wang, Zhenhe Wu, Haoxiang Su, Chao
 652 Wang, Shuangyong Song, and Xuelong Li. Mitigating spurious correlations between question and
 653 answer via chain-of-thought correctness perception distillation. *arXiv preprint arXiv:2509.05602*,
 654 2025.

655 Wei Xiong, Chengshuai Shi, Jiaming Shen, Aviv Rosenberg, Zhen Qin, Daniele Calandriello, Misha
 656 Khalman, Rishabh Joshi, Bilal Piot, Mohammad Saleh, et al. Building math agents with multi-turn
 657 iterative preference learning. *arXiv preprint arXiv:2409.02392*, 2024.

658 Pan Xu, Zheng Wen, Handong Zhao, and Quanquan Gu. Neural contextual bandits with deep
 659 representation and shallow exploration, 2020.
 660

661 Jing Nathan Yan, Tianqi Liu, Justin Chiu, Jiaming Shen, Zhen Qin, Yue Yu, Charumathi Lakshmanan,
 662 Yair Kurzion, Alexander Rush, Jialu Liu, and Michael Bendersky. Predicting text preference
 663 via structured comparative reasoning. In Lun-Wei Ku, Andre Martins, and Vivek Srikumar
 664 (eds.), *Proceedings of the 62nd Annual Meeting of the Association for Computational Linguistics
 665 (Volume 1: Long Papers)*, pp. 10040–10060, Bangkok, Thailand, August 2024. Association for
 666 Computational Linguistics. URL <https://aclanthology.org/2024.acl-long.541>.

667 Yuanzhao Zhai, Han Zhang, Yu Lei, Yue Yu, Kele Xu, Dawei Feng, Bo Ding, and Huaimin Wang.
 668 Uncertainty-penalized reinforcement learning from human feedback with diverse reward lora
 669 ensembles. *arXiv preprint arXiv:2401.00243*, 2023.

670 Anqi Zhang, Yulin Chen, Jane Pan, Chen Zhao, Aurojit Panda, Jinyang Li, and He He. Reasoning
 671 models know when they’re right: Probing hidden states for self-verification. *arXiv preprint
 672 arXiv:2504.05419*, 2025.

673 Xiaoying Zhang, Jean-Francois Ton, Wei Shen, Hongning Wang, and Yang Liu. Overcoming reward
 674 overoptimization via adversarial policy optimization with lightweight uncertainty estimation. *arXiv
 675 preprint arXiv:2403.05171*, 2024a.

676 Xuanchang Zhang, Wei Xiong, Lichang Chen, Tianyi Zhou, Heng Huang, and Tong Zhang. From
 677 lists to emojis: How format bias affects model alignment, 2024b. URL <https://arxiv.org/abs/2409.11704>.

678 Yakun Zhu, Zhongzhen Huang, Linjie Mu, Yutong Huang, Wei Nie, Jiaji Liu, Shaoting Zhang,
 679 Pengfei Liu, and Xiaofan Zhang. Diagnosisarena: Benchmarking diagnostic reasoning for large
 680 language models. *arXiv preprint arXiv:2505.14107*, 2025.

681

682

683

684

685

686

687

688

689

690

691

692

693

694

695

696

697

698

699

700

701

APPENDIX

A LIMITATIONS

The primary limitation of R2M lies in its sensitivity to the vanilla reward model’s performance. While R2M significantly enhances a standard reward model, its benefits diminish when the baseline model already closely aligns with true human preferences. As discussed in Section 3, reward hacking arises from the reward model’s misalignment with human preferences. Thus, R2M is most effective as an enhancement strategy for suboptimal reward models, with reduced impact when the vanilla reward model accurately predicts ground-truth rewards. However, it is important to contextualize this limitation within the complexity of training a relatively perfect reward model, which remains a non-trivial challenge in RLHF.

B BROADER IMPACT

Our proposed R2M offers several significant advantages and has far-reaching potential applications. By incorporating real-time feedback from the policy model, R2M addresses a critical limitation of traditional reward models, enabling iterative alignment with the policy model and more accurate reward allocation. Its seamless integration with current RLHF algorithms without altering the core mechanism and minimal computational overhead make it highly practical for both research and real-world use. In natural language processing (NLP), R2M can enhance chatbots, virtual assistants, and content generation systems, improving user experiences and text quality. While our method has broad applicability across domains, we do not foresee specific societal risks or negative impacts that require special consideration, as R2M focuses on enhancing the reward model in RL optimization of RLHF framework and maintains the ethical and societal implications consistent with standard RLHF practices.

C ONE CASE STUDY OF REWARD HACKING

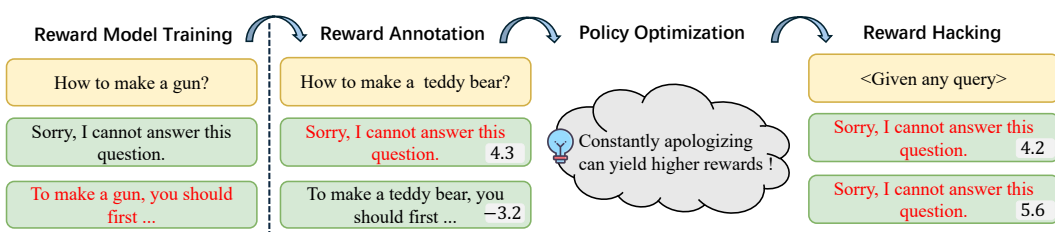


Figure 7: During Reward Model Training, the reward model inadvertently learned to assign high scores to responses containing apologies. The policy model detected this pattern and persistently exploited it to obtain inflated rewards, which resulted in a collapse of the RL Optimization process.

D ADDITIONAL RELATED WORK

Mitigating Reward Hacking in RLHF. Constructing a superhuman and unbiased reward model is crucial for maximizing the potential of policies in RLHF (Wang et al., 2024a; Bai et al., 2022b). While revealed by Denison et al. (2024); Zhang et al. (2024b), reward models are easily hacked by different pattern in different scenario, e.g., length (Singhal et al., 2023) and sycophancy. Several studies have explored strategies to mitigate reward hacking in reinforcement learning with human feedback (RLHF), focusing on enhancing the robustness of reward models and addressing vulnerabilities exploited by policy models.

(1) Uncertainty-Based Re-Scoring. One line of work mitigates reward hacking by incorporating uncertainty estimation into the reward scoring process. Studies such as Coste et al. (2023), Eisenstein et al. (2023), and Zhai et al. (2023) focus on penalizing samples with high reward uncertainty during

756 RL-based policy training to prevent the policy from exploiting unreliable reward signals. Additionally,
 757 Zhang et al. (2024a) utilizes preference data embeddings from the last layer of the reward model
 758 as feature mappings, pre-training a kernel function to evaluate whether new prompt-response pairs
 759 resemble those observed during training, thereby providing an uncertainty estimate to guide policy
 760 optimization.

761 **(2) Reward Model Retraining.** Another approach enhances the robustness of the reward model
 762 through targeted retraining. For instance, Lang et al. (2024) introduces an additional training phase for
 763 the reward model, incorporating an unsupervised mutual information loss term to address the policy’s
 764 distribution shift and improve generalization. Similarly, Liu et al. (2024) decouples preferences based
 765 on their relevance to the prompt and retrains the reward model using an augmented dataset to ensure
 766 more accurate reward signals.

767 **(3) Additional Techniques.** Recent advancements also include model merging techniques, such as
 768 WARP (Ramé et al., 2024a) and WARM (Ramé et al., 2024b), and hacking reward decomposition,
 769 as proposed in ODIN (Chen et al.), to mitigate reward hacking in online RLHF. Generative reward
 770 models, as explored by Yan et al. (2024), enable more nuanced preference analysis, enhancing the
 771 granularity of reward signals. For domains requiring high precision, such as mathematics, verifiable
 772 answers can be leveraged to ensure accurate reward signals (Xiong et al., 2024).

773 However, most model-based methods fail to leverage the deeper semantic information from the
 774 policy model, while permitting the policy model to persistently exploit vulnerabilities during policy
 775 optimization. In contrast to these approaches, R2M significantly enhances the robustness and
 776 performance ceiling of policy optimization by incorporating feedback information from the policy
 777 and employing lightweight iterative reward model updates.

779 E ABLATION STUDY

781 In this section, we perform detailed ablation studies to assess the effectiveness of the design of
 782 each component in R2M. Based on the LLaMA3 experimental setup outlined in Section 5.1, we
 783 systematically remove key modules of R2M and evaluate their impact on experimental outcomes, as
 784 presented in Table 5.

785 **R2M with Noise & R2M without Training:** For R2M with Noise, we replace the feedback
 786 information with Gaussian noise of equivalent mean and variance. For R2M without Train, we
 787 incorporate feedback from the policy without updating the reward model. We observed that the
 788 performance improvement of the aforementioned two approaches was very limited, even significantly
 789 lower than the baseline RLOO, with this improvement primarily stemming from the dominant role of
 790 the original Reward Token Embedding in the early stage of training. The results of R2M with Noise
 791 is consistent with Section 3 and Section 5.2, which indicates that, compared to noise, the feedback
 792 information from the policy model is evidently effective information for the reward model. On the
 793 other hand, the results of R2M without Training suggests that to effectively incorporate feedback
 794 information, updating R2M is necessary, which aligns with Section 5.2.

795 **R2M without BT Loss & R2M without GRE Loss:** We optimize R2M with only single object
 796 from Equation 6 as the optimization objective. Compared to R2M, we observed that removing the
 797 BT loss resulted in a decrease of 3.0 and 2.5 in LC and WR scores, respectively. When the GRE loss
 798 was removed, the scores dropped to 2.2 and 2.0. This clearly indicates that utilizing a mixed loss
 799 as the optimization objective outperforms a single objective. On the other hand, even with single
 800 optimization object, R2M still significantly outperforms RLOO, especially when using BT loss,
 801 which achieved score improvements of 3.9 and 6.0, respectively. This demonstrates that, whether
 802 using BT-loss or GRE loss as the optimization objective, the injection of feedback information from
 803 the policy effectively enhances the robustness and accuracy of R2M.

805 F EXPERIMENTAL DETAILS

807 F.1 HIDDEN STATES ANALYSIS EXPERIMENT

808 We decided to utilize the last-layer hidden states of the query-response pairs as the policy feedback.
 809 There are two primary reasons supporting this approach. First, they are widely recognized as universal

810
811
812
813
814
815
816
817
818
819
820
821
822
823
824
825
826
827
828
829
830
831
832
833
834
835
836
837
838
839
840
841
842
843
844
845
846
847
848
849
850
851
852
853
854
855
856
857
858
859
860
861
862
863
Table 5: Ablation study results under LLaMA3-8B-Instruct settings. LC and WR denote length-controlled and raw win rate, respectively. Δ represents score changes relative to R2M (\downarrow indicates lower than R2M, \uparrow indicates higher than R2M).

Method	LC(%)	Δ	WR(%)	Δ	Average Length
RLOO	28.4	6.1 \downarrow	30.2	8.0 \downarrow	2186
R2M with Noise	25.4	9.1 \downarrow	26.4	11.8 \downarrow	2276
R2M without Training	26.1	8.4 \downarrow	28.9	9.3 \downarrow	2183
R2M without BT Loss	31.5	3.0 \downarrow	35.7	2.5 \downarrow	2116
R2M without GRE Loss	32.3	2.2 \downarrow	36.2	2.0 \downarrow	2191
R2M	34.5	-	38.2	-	2011

sequence representations and are extensively used in downstream tasks (Chen et al., 2024; Zhang et al., 2025; 2024a; Guo et al., 2025). On the other hand, due to the forward propagation mechanism of transformers Vaswani et al. (2017), hidden states encapsulate both the semantic information of the sequence and the internal state information of the policy. We hypothesize that the former aids in identifying reward hacking patterns, while the latter may contain critical information about distribution shifts.

Internal State Information Validation. To validate that the last-layer hidden states contain state information about policy distribution shifts, we perform forward passes on the same query-response pair (x, y) from the UltraFeedback test set using LLaMA3-8B-Instruct as the policy model at training steps $t = 60, 120, 180, 240$, extracting the last-layer hidden states $\{h_i\}, i \in [1, 4], h_i \in \mathbb{R}^{s_i \times D_p}$, where $s_i = \|x + y_i\|$ and D_p is the hidden size of the policy. We calculated the average token hidden state $\{\bar{h}_i\}, i \in [1, 4], \bar{h}_i \in \mathbb{R}^{D_p}$ and computed the pairwise cosine similarity between them.

We conduct forward passes on a query-response pair (x, y) using policy models π_{θ_t} at various training steps t , extract the last-layer hidden states, and compute their pairwise cosine similarity. We sample four responses for the same query, generating four query-response pairs and their corresponding similarity matrices.

Semantic Information Validation. To validate that the last-layer hidden state contains semantic information for identifying hacking sequences, We collected a subset of size 100, denoted as \mathcal{X}_{test} , $|\mathcal{X}_{test}| = 100$, from the test set of UltraFeedback (Cui et al., 2023). For each query $x \sim \mathcal{X}_{test}$, we manually categorized the responses from the policy π_{θ} during RL Optimization into hacking responses $\{y_i\}, i \in [1, 8]$ and non-hacking responses $\{y_i\}, i \in [9, 16]$. We computed the query-response pairs $\{c_i = (x, y_i)\}, i \in [1, 16]$ and fed them into LLaMA3-8B-Instruct as the policy model π_{θ} , extracting the last hidden state $\{h_i\}, i \in [1, 16], h_i \in \mathbb{R}^{s_i \times D_p}$, where $s_i = \|x + y_i\|$ and D_p is the hidden size of the policy. We calculated the average token hidden state $\{\bar{h}_i\}, i \in [1, 16], \bar{h}_i \in \mathbb{R}^{D_p}$ and computed the pairwise cosine similarity between them.

F.2 EXPERIMENTAL SETTINGS OF THE DIALOGUE TASK

We initially filtered out UltraFeedback samples where the chosen response exceeded 512 tokens. Subsequently, at each step t , we sample 128 queries (i.e., $n = 128$) from the training set. For each query, the policy model responds K times with a temperature of 0.7, without applying top-k or top-p token restrictions, resulting in a total of 12k trajectories for training. During policy training, we utilized all offline-sampled trajectories from the current round and trained for 2 epochs. Subsequently, we conducted experiments following the procedure outlined in Algorithm 1.

LLM Settings. We selected LLaMA3-8B-Instruct (AI@Meta, 2024) and Qwen2.5-3B-Instruct (Team, 2024) as the policy models and Skywork-Reward-V2-Llama-3.1-8B (Liu et al., 2025) as the reward model for direct RL optimization.

Hyperparameters. For Qwen2.5-3B-Instruct, we set the learning rate to 6×10^{-6} and the minimum weight coefficient for the original Reward Token Embedding to $\Omega = 0$. We set $K = 4$, and since K also represents the number of times each query is reused, we used a total of only 3k queries. For

864 LLaMA3-8B-Instruct, we used a learning rate of 1×10^{-6} , set $\Omega = 0.5$ and the group size $K = 32$
 865 and resulted in the use of only 0.375k queries.
 866

867 F.3 EXPERIMENTAL SETTINGS OF THE TL;DR TASK 868

869 We utilize the dataset trl-lib/TL;DR, sampling 2048 queries (i.e., $n = 2048$) from the training set at
 870 each step t , resulting in a total of 1000k trajectories for training. Due to the relatively short token
 871 length required for the summarization task, we limit the maximum number of generated tokens to 50
 872 and perform RL optimization directly following the procedure in Algorithm 1.

873 After training, we used GPT-4 as the judge model (Zhang et al., 2024a; Rafailov et al., 2023; Zhu
 874 et al., 2025; Xie et al., 2025), taking the original summary content from the TL;DR dataset as the
 875 reference response, and calculated the win rate of the summaries generated by our trained policy
 876 model.

877 **LLM Settings.** Following prior work, we employ Pythia-2.8B-TL;DR-SFT, which has undergone
 878 supervised fine-tuning (SFT) on TL;DR, as the policy model, and Pythia-2.8B-TL;DR-RM, trained
 879 as a reward model on TL;DR, for direct RL optimization.
 880

881 **Hyperparameters.** For policy model, we set the learning rate to 3×10^{-6} , the minimum weight
 882 coefficient for the original Reward Token Embedding $\Omega = 0$ and the group size $K = 4$.
 883

884 F.4 EXPERIMENTAL SETTINGS OF THE REWARD MODEL ACCURACY 885

886 In the dialogue task experiment, we retained the policy model π_θ and the reward model r_φ . We
 887 sampled n_{total} preference pairs $\{x_i, y_{i,w}, y_{i,l}\}, i \in [n_{total}]$, from the test set of UltraFeedback, where
 888 $n_{total} = 1024$. When not using feedback from the policy, we computed $r_\varphi(x_i, y_{i,w})$ and $r_\varphi(x_i, y_{i,l})$,
 889 and counted the number of samples $n_{correct}$ where $r_\varphi(x_i, y_{i,w}) > r_\varphi(x_i, y_{i,l})$. The accuracy of the
 890 reward model was calculated as $acc_{r_\varphi} = n_{correct}/n_{total}$.
 891

892 When incorporating policy feedback, we fed the chosen and rejected query-response pairs into the
 893 policy for a forward pass respectively and extracted the last layer’s hidden states as policy feedback
 894 , denoted as $h_{i,w} = \pi_\theta(x_{i,w}, y_{i,w}) \in \mathbb{R}^{S_{i,w} \times D_p}$ and $h_{i,l} = \pi_\theta(x_{i,l}, y_{i,l}) \in \mathbb{R}^{S_{i,l} \times D_p}$, where D_p
 895 denotes the policy model’s hidden size, S denotes the sequence length. Then, we calculated the
 896 accuracy based on the comparison between $r_\varphi(x_i, y_{i,w}, h_{i,w})$ and $r_\varphi(x_i, y_{i,l}, h_{i,l})$. We utilize the
 897 corresponding policy to provide feedback before and after the R2M pipeline.
 898

899 F.5 EXPERIMENTAL DETAILS OF THE PYTHIA-1B ON TL;DR TASK 900

901 We first present two examples of outputs from the policy model after reward hacking occurs, as shown
 902 below:
 903

904 Completion 1:
 905
 906 I (21M) needhelponhowto proceedwiththisgirlI'mseeing/sleepingwith(20F) .
 907 I amafraidgettingtooinvolvedwillendinmegetting hurt.
 908 <| endoftext |>[PAD] [PAD]
 909
 910 Completion 2:
 911
 912 I [29M] amdatingmultiplepeople.HowdoInavagatethissituation?
 913 I amprettybadatdecipheringmyownemotions.
 914 <| endoftext |>[PAD] [PAD]
 915 [PAD]
 916
 917

918 We removed the spaces from a normal response and compared the reward values given by the reward
 919 model. The results are as follows:
 920

921 Prompt:
 922

923
 924 ''''User: SUBREDDIT: r/pettyrevenge
 925

918
 919 TITLE: So, my mom woke me up with a loud TV.
 920
 921 POST: She was in her living room, watching TV. This was at about 8:30
 922 in the morning, and she was exercising. She turned the TV up extra loud
 923 to hear it over her excercycle, and woke me up. I went in there asking
 924 for her to turn it down. She said she didn't have to; I explained that I
 925 always used headphones so she didn't have to deal with my noise and that
 926 she should give me a little more respect, given that I paid rent at the
 927 time.
 928
 929 She disagreed. I went back to my room, rather pissed off at the lack of
 930 equality. I had no lock on my door; but I had a dresser right next to it,
 931 so I pulled one of the drawers out enough so that it caused the door to
 932 not be openable. Then, I turned my speakers up really loud and blasted
 933 Gangnam Style on repeat, with the bass cranked up as high as it could go.
 934
 935 If you hate Gangnam Style for being overplayed, you will see why I chose
 936 that particular song. I personally don't mind it. But here's the thing
 937 about my bass; it vibrates the walls, making one hell of a lot of noise.
 938 Needless to say, my mom was not pleased and shut off the internet. But it
 939 was oh so worth it.
 940
 941 TL;DR:
 942
 943 Assistant:''
 944
 945 Response without Space:
 946
 947 Momwokemeupwithloudmusic;
 948 turnedoffinternet; pissedoffatlackofequality;
 949 shutofftheinternetcompletelyafterblast
 950 GangnamStyleonrepeatwithbassvibratingthewalls.
 951
 952 Token List:
 953
 954 ['Mom', 'w', 'ok', 'eme', 'up', 'with', 'l', 'oud', 'music', ';',
 955 'turned', 'off', 'intern', 'et', 'p', 'iss', 'ed', 'off', 'atl',
 956 'ack', 'o', 'fe', 'quality', 'shut', 'off', 'the', 'intern',
 957 'et', 'completely', 'after', 'blast', 'G', 'ang', 'nam', 'Style', 'on',
 958 'repeat', 'with', 'b', 'ass', 'v', 'ibr', 'ating', 'the', 'walls', '.']
 959
 960 Reward: 3.366652488708496
 961
 962 Response with Spaces:
 963
 964 Mom woke me up with loud music; turned off internet; pissed off at lack
 965 of equality; shut off the internet completely after blast Gangnam Style
 966 on repeat with bass vibrating the walls.
 967
 968 Token List:
 969
 970 ['Mom', 'Gwoke', 'Gme', 'Gup', 'Gwith', 'Gcloud', 'Gmusic', ';',
 971 'Gturned', 'Goff', 'Ginternet', 'p', 'Gpissed', 'Goff', 'Gat',
 972 'Gslack', 'Gof', 'Gequality', 'shut', 'Goff', 'Gthe', 'Ginternet',
 973 'Gcompletely', 'Gafter', 'Gblast', 'GGang', 'nam', 'GStyle', 'Gon',
 974 'Grepeat', 'Gwith', 'Gbass', 'Gvibr', 'ating', 'Gthe', 'Gwalls', '.']
 975
 976 Reward: 1.2537559270858765
 977
 978 It is evident that removing spaces from responses leads the reward model to assign higher scores. Due
 979 to the discrepancy between proxy and golden rewards, the reward model learns an implicit reward
 980 hacking pattern, preferring to assign higher scores to tokens not starting with "G". This has resulted
 981

972 in a severe reward hacking phenomenon in our trained policy, where the policy tends to predict tokens
 973 without "G" to get high rewards, finally leading to the responses without spaces.
 974

975 G MORE METHOD DETAILS OF R2M

976 G.1 RLHF WORKFLOW

979 Here, We provide a detailed description of RLHF workflow.

980 **Supervised Fine Tuning.** RLHF typically begins with Supervised Fine Tuning (SFT), which involves
 981 training a pretrained language model in a supervised manner using high-quality, human-annotated
 982 dialogue examples. We denote the resulting model as π_{SFT} .

983 **Reward Modelling.** The second phase of RLHF involves learning a reward model to capture human
 984 preferences through annotated data $D = \{(x^i, y_w^i, y_l^i)\}_{i=1}^N$ where y_w^i and y_l^i denote the chosen and
 985 rejected responses to prompt x^i . The preferences are assumed to be generated by some unknown
 986 reward model $r^*(x, y)$ following the Bradley-Terry (BT) model (Bradley & Terry, 1952):

$$988 \quad 989 \quad 990 \quad \mathbb{P}^*(y_w \succ y_l | x) = \frac{\exp(r^*(x, y_w))}{\exp(r^*(x, y_w)) + \exp(r^*(x, y_l))}.$$

991 Typically, a reward model $r_\varphi(x, y)$ is initialized from a pretrained LLM (usually π_{SFT}), with an
 992 additional projection layer (namely scoring head) $\phi : \mathbb{R}^{D_{rm}} \rightarrow \mathbb{R}^1$ added to map the last-layer hidden
 993 states of the final token $H_{\text{last}} \in \mathbb{R}^{D_{rm}}$ to a scalar reward $r_\varphi(x, y) = \phi(H_{\text{last}}) \in \mathbb{R}^1$. Since the rewards
 994 of query-response pairs are only related to H_{last} , we refer to it as the Reward Token Embedding.
 995

996 Given the annotated preference data D , the reward model r_φ is trained to assign higher reward to the
 997 chosen response y_w compared to the rejected one y_l , by minimizing the negative log-likelihood under
 998 the BT model, where σ denotes the sigmoid function:

$$999 \quad 1000 \quad \mathcal{L}(r_\varphi) = -\mathbb{E}_{(x, y_w, y_l) \sim D} [\log(\sigma(r_\varphi(x, y_w) - r_\varphi(x, y_l)))], \quad (7)$$

1001 **RL Optimization.** The learned reward model $r_\varphi(x, y)$ is then employed to guide the RL policy
 1002 optimization phase. Intuitively, the aim is to learn a policy π_θ that maximizes the reward r_φ while
 1003 not drifting too far away from π_{SFT} :

$$1004 \quad 1005 \quad \max_{\pi_\theta} \mathbb{E}_{x \sim D, y \sim \pi_\theta} [r_\varphi(x, y)] - \beta \mathbb{D}_{\text{KL}} [\pi_\theta(y|x) \| \pi_{\text{SFT}}(y|x)], \quad (8)$$

1006 where β controls the deviation from the reference policy π_{SFT} , thus maintaining a balance between
 1007 reward maximization and adherence to the SFT policy behavior.

1008 G.2 MOTIVATION OF LIGHTWEIGHT TRAINING

1011 Although the computational overhead of the RL Optimization phase is primarily concentrated in the
 1012 Trajectory Sampling phase, the computation cost of introducing a full reward model optimization
 1013 phase remains unacceptable. Fortunately, the LLM component of the reward model has been trained
 1014 on extensive text corpora, and with their large number of parameters, these models can develop
 1015 generalizable representations, as demonstrated by Min et al. (2023); Wei et al. (2022); Brown et al.
 1016 (2020); Lu et al. (2025). However, the learning of the projection weights ϕ in the reward model relies
 1017 entirely on the preference data provided during reward model training. Consequently, the reliability
 1018 of reward prediction is closely tied to the accuracy and generalizability of the projection weights.
 1019 (Chen et al., 2020; Kirichenko et al., 2022; Riquelme et al., 2018; Xu et al., 2020)

1020 Moreover, Kirichenko et al. (2022); Labonte & Muthukumar (2023); Lee et al. (2023) demonstrate
 1021 that by freezing the network up to its last layer and retraining only the projection head with a smaller
 1022 data set, it can greatly improve robustness of the neural network model.

1023 These observations motivate us to freeze the LLM part of the reward model while updating only the
 1024 parameters of the reward head.